Japanese Journal of Applied Physics
Vol. 44, No. 11, 2005, pp. 8027–8031
©2005 The Japan Society of Applied Physics

Investigation of Transparent Conductive Oxide Al-Doped ZnO Films Produced by Pulsed Laser Deposition

Sang-Moo PARK*, Tomoaki IKEGAMI and Kenji EBIHARA[1]

Graduate School of Science and Technology, Kumamoto University, 2-39-1 Kurokami, Kumamoto 860-8555, Japan
[1]*Department of Electrical and Computer Engineering, Kumamoto University, 2-39-1 Kurokami, Kumamoto 860-8555, Japan*

(Received May 24, 2005; accepted July 27, 2005; published November 9, 2005)

High-quality transparent conductive aluminum-doped ZnO (AZO) thin films were deposited on quartz glass substrates using pulsed laser deposition (PLD). We varied the growth conditions in terms of substrate temperature and oxygen pressure. The crystallographic structure and electrical and optical properties of the as-grown AZO films were mainly investigated. In X-ray diffraction (XRD), (002) and (004) peaks were detected, indicating that Al doping did not cause structural degradation of wurtzite ZnO. The AZO films formed at a substrate temperature of 300°C showed a low electrical resistivity of $1.33 \times 10^{-4}\,\Omega\,\mathrm{cm}$, a carrier concentration of $1.25 \times 10^{21}\,\mathrm{cm}^{-3}$ and a carrier mobility of $37.6\,\mathrm{cm}^2/(\mathrm{V\,s})$ at an oxygen pressure of 5 mTorr. A visible transmittance of above 88% was obtained. The AZO films show comparable electrical and optical properties to those of indium tin oxide (ITO) films and are emerging as a potential good challenger to ITO films.
[DOI: 10.1143/JJAP.44.8027]

KEYWORDS: ZnO, Al-doped ZnO, transparent conductive oxide, electric and optical properties, pulsed laser deposition

1. Introduction

Zinc oxide (ZnO) is a II–VI semiconductor, highly transparent in the visible region with a wide and direct band gap of about 3.37 eV at room temperature and a high exciton binding energy of 60 meV.[1)] This material is very attractive because it has many applications such as transparent conductive contacts, solar cells, laser diodes, ultraviolet lasers and thin-films transistors.[2–6)] Undoped ZnO thin films generally typically exhibit *n*-type conduction with a background electron concentration as high as $10^{21}\,\mathrm{cm}^{-3}$. The Al-doped ZnO (AZO) film exhibits remarkable electrical conductivity together with a high charge carrier density of $10^{21}\,\mathrm{cm}^{-3}$ and a mobility of $30\,\mathrm{cm}^2/(\mathrm{V\,s})$.[7,8)] AZO films can be used as thin-film solar cells, electrodes for flat panel displays and anodes for organic light emitting diodes.[9,10)] ZnO is an oxide that can be grown as a thin film by many deposition techniques including chemical vapor deposition, radio frequency sputtering, magnetron sputtering, sol–gel, ion-beam-assisted molecular-beam epitaxy, and pulsed laser deposition.[11–14)] Among the several fabrication techniques, pulsed laser deposition (PLD) has attracted much attention because the fabrication process is quite suitable for optoelectronic devices using the ZnO transparent electrode. The composition of films grown by PLD is quite close to that of the target, even for a multi component target. PLD films may be crystallized at deposition temperatures lower than those of other physical vapor deposition techniques due to the high kinetic energies of the ionized and ejected species in the laser plumes.[15)] However, it is difficult to make the transparent layer on the optoelectronic devices because the electrical and optical properties of AZO films vary markedly depending on the PLD conditions. In this work we report results obtained from AZO films grown by KrF excimer PLD at different substrate temperatures and background pressures of oxygen gas. The crystallographic structure and the optimization of the electrical and optical properties of the films prepared with different growth parameters will be discussed.

*E-mail address: smpark@st.eecs.kumamoto-u.ac.jp

2. Experimental

A detailed description of the PLD system is reported elsewhere.[16)] Transparent conductive AZO films were prepared by pulsed laser deposition on quartz glass substrates. The pulsed laser was a KrF excimer laser ($\lambda = 248\,\mathrm{nm}$, 25 ns pulse width) with an energy fluence of $2\,\mathrm{J/cm}^2$. The AZO films were prepared by ablating a ZnO target containing 2 wt% Al_2O_3. A substrate was placed 40 mm away from the target and could be heated up to 1000°C. The typical growth run consisted of 9,000 laser shots with a repetition rate of 10 Hz. All of the films were also deposited on quartz glass cleaned in an ultrasonic bath using acetone and then ethanol for 5 min. The deposition chamber was initially evacuated to 4×10^{-5} Torr and during deposition, oxygen gas was introduced into the growth chamber and the pressure was controlled to be 1–100 mTorr using a conductance valve and a turbo molecular pump. The as-grown AZO films were characterized by X-ray diffraction (XRD, Rigaku, RINT 2100/PC). The surface morphology was observed by atomic force microscopy (AFM, Seiko Instrument, SPI 3800N). The growth rate and the thickness of the sample were determined by cross-sectional scanning electron microscopy (SEM, JEOL JSM-T200). Transmission through the films was measured using a UV–visible spectrophotometer in the wavelength range from 200–800 nm. The electrical properties of the AZO films were measured by the van der Pauw method at room temperature.

3. Results and Discussion

3.1 Study as a function of oxygen pressure

The resulting XRD patterns of Al-doped ZnO exhibit two diffraction peaks observed at around 34.58° (002) and 72.66° (004). The Al peak cannot be seen, because only 2 wt% Al_2O_3 was doped. They show the characteristic of the hexagonal ZnO wurtzite, the *c*-axis being perpendicular to the substrate plane.[17)] Figure 1 shows the effect of oxygen pressure (p_{O_2}) on the crystallinity of the AZO films. The ambient oxygen pressure was changed from 1 to 100 mTorr at a substrate temperature of 500°C. XRD 2θ scans in the vicinity of the ZnO(002) reflection were performed on these

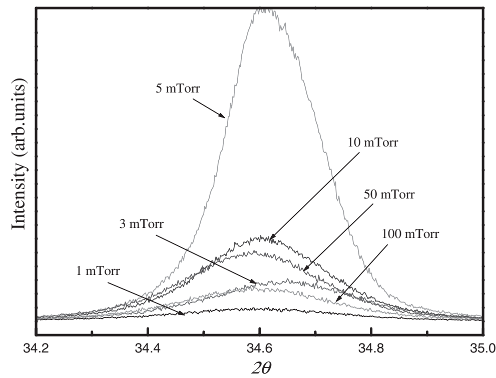

Fig. 1. XRD patterns for AZO films grown on quartz glass substrates at 500°C as a function of oxygen pressure.

films. A strong peak signal of the (002) diffraction was observed for the 5 mTorr film, while the film prepared at 1 mTorr shows clear evidence of crystallinity.

Figure 2(a) shows that the full width at half maximum (FWHM) of XRD (002) peaks is decreasing from 0.332° at 1 mTorr to 0.198° at 5 mTorr. The peak intensity shows a marked increase with p_{O_2} up to 100 mTorr. Additional information is given from the XRD measurements by calculating the crystal size of ZnO film using Scherrer's formula[18]

$$D = \frac{0.9\lambda}{\beta \cos\theta}, \tag{1}$$

where λ is the X-ray wavelength (1.5402 Å), β is the (002) peak width (in radians), D is the crystal size, and θ is the Bragg diffraction angle. Table I shows that the crystal size increases from 10.15 nm at 1 mTorr to 34.02 nm at 5 mTorr, and then decreases gradually for samples prepared at up to 100 mTorr. These findings suggest that the crystalline quality of the AZO films degraded from a single-oriented crystal to polycrystalline with the increase in oxygen content. The excess oxygen might have induced defects in the films, which influenced the nucleation and growth of the films and resulted in the degradation of the crystalline quality (see also Table I). These results also confirm that a pressure of 5 mTorr will give better epitaxy (as seen from 2θ scan), better texture (as seen from the FWHM values), and a larger crystal size (34 nm using Scherrer's formula) for the AZO films.

The optical transmittance measurements between 200 and 800 nm show that the films are highly transparent in the visible region and present a steep decline at around 380 nm. This optical transmittance can be used to determine the value

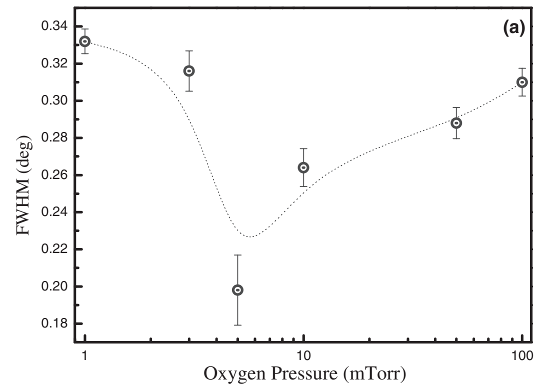

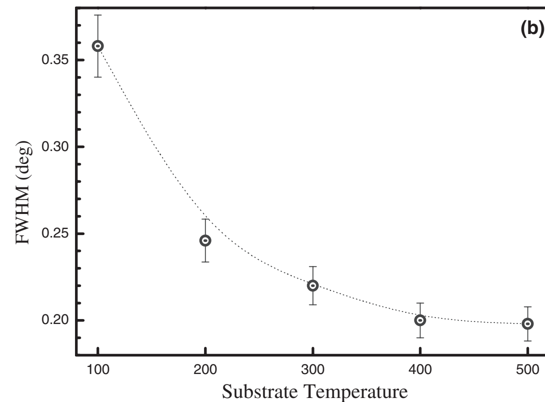

Fig. 2. FWHM of 2θ scan plotted as a function (a) of oxygen pressure (for deposition temperature of 500°C) and as a function (b) of deposition temperature (for oxygen pressure of 5 mTorr).

of the optical band gap. The optical band gap was calculated from the transmittance data by using Tauc's plot. Figure 3 shows the shift of the optical band gaps of ZnO and AZO films. The high-energy shift of the optical band gap of the AZO films compared with that of the ZnO films is due to the much higher carrier concentration and the filling of electronic states of the conduction band (Burstein–Moss-shift) in the AZO films.[19]

Figure 4 shows the variations in resistivity, carrier concentration, and carrier mobility as functions of oxygen pressure for the AZO deposited at a deposition temperature of 500°C. The films thickness was about 2000 Å for all films. The resistivity of the AZO films decreases from 5.14×10^{-4} to $3.92 \times 10^{-4}\,\Omega\,\mathrm{cm}$ as the p_{O_2} was increased from 1 to 5 mTorr. The initial decrease in resistivity with increase in p_{O_2} can be attributed to an increase in the crystal size of the AZO film from 10.15 to 34.05 nm, thus reducing the grain boundary scattering and increasing the conductivity. A rapid

Table I. Properties of AZO film on quartz glass substrates at 500°C as functions of oxygen pressure.

p_{O_2} (mTorr)	Crystal size (nm)	c-axis length (Å)	Roughness (nm)	T (%) (400–800 nm)	Band gap (eV)	Resistivity (Ω cm)	Carrier concentration (cm^{-3})	Carrier mobility [$\mathrm{cm}^2/(\mathrm{V\,s})$]
1	10.15	5.178	7.062	88.66	3.36	5.14×10^{-4}	1.25×10^{21}	9.74
3	22.8	5.173	7.142	90.97	3.36	4.97×10^{-4}	1.16×10^{21}	10.87
5	34.02	5.176	7.97	93.37	3.35	3.92×10^{-4}	1.14×10^{21}	14.03
10	25.3	5.182	7.354	95.46	3.34	7.5×10^{-4}	1.04×10^{21}	8.01
50	23.5	5.187	7.227	94.63	3.32	1.78×10^{-3}	9.92×10^{20}	3.55
100	21.3	5.185	6.834	95.14	3.26	5.22	1.25×10^{19}	0.1

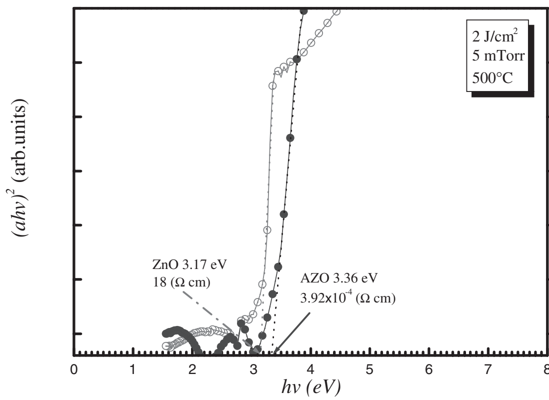

Fig. 3. Tauc's plot of transparencies in optical properties of ZnO and AZO thin films prepared at substrate temperature of 500°C and at oxygen pressure of 5 mTorr.

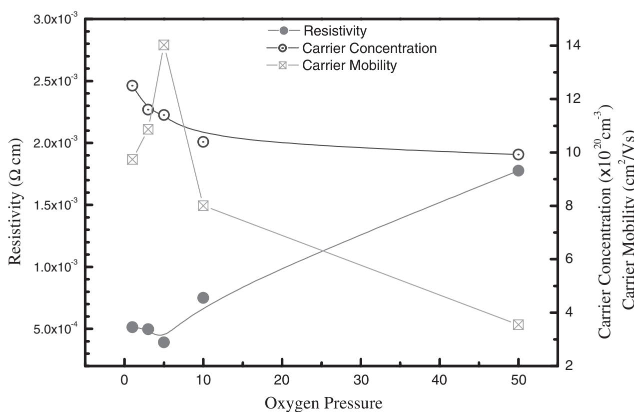

Fig. 4. Variations in resistivity, carrier concentration, and carrier mobility as functions of oxygen pressure for AZO deposited at deposition temperature of 500°C.

increase in resistivity is observed as p_{O_2} is further increased from 5 to 100 mTorr. The electrical properties of AZO films have close relationship to oxygen content in the films. AZO is an oxide semiconductor having *n*-type conduction. The high conductivity of AZO might be an effect of Al-doping. Since electrons in the AZO films are supplied from oxygen vacancies and aluminum atoms in the film, it can be though that an increase in oxygen content might cause a decrease in the number of oxygen vacancies, resulting in an increase of resistivity. With increasing p_{O_2}, the optical band gap is gradually decreased from 3.36 to 3.26 eV by the relaxation of built-in strain in AZO (see also Table I). According to the Burstein–Moss effect, the broadening of the optical band gap is

$$\Delta E_g = \left(\frac{\hbar^2}{2m^*_{cv}}\right)(3\pi^2 n)^{2/3}, \qquad (2)$$

where ΔE_g is the shift of the doped semiconductor with respect to the undoped semiconductor, m^*_{cv} is the reduced effective mass, $\hbar$ is Plank's constant and n is the carrier concentration. According to this equation, the band gap would increases with carrier concentration. Carrier concentration in the AZO films was observed to gradually decrease from 1.36×10^{21} to 9.92×10^{20} cm^{-3} as oxygen pressure was increased. A maximum in carrier mobility was observed for an oxygen pressure of 5 mTorr. For lower ratios of O and Zn (oxygen flow rates of 1–5 mTorr), incorporation of interstitial Zn led to a worsening of crystalline quality and creation of electron scattering centers. Consistent with this, carrier mobility was found to increase with increasing oxygen flow rate below the optimum oxygen pressure of 5 mTorr. For ratios of O and Zn higher than that corresponding to the optimum oxygen pressure of 5 mTorr, excess oxygen on the growth surface presumably induces changes in growth mode and crystal quality, resulting in increased carrier scattering and lower mobility. Carrier mobility thus decreases with increasing oxygen pressure of 5 mTorr.

These experiments suggest that at a substrate temperature of 500°C, the oxygen pressure should be 5 mTorr. Thus, for the second time, we have investigated the effect of the substrate temperature for a fixed p_{O_2} of 5 mTorr.

3.2 Study as a function of deposition temperature

A series of films grown in 5 mTorr of O_2 were investigated by varying the substrate temperature. The XRD spectra of the AZO films deposited are shown in Fig. 5. Two diffraction peaks corresponding to (002) and (004) reflections are predominant and indicate that the film has a *c*-axis direction with an out-of-plane lattice parameter of around 5.2 Å. At higher substrate temperatures the intensity of (002) peaks increased. The FWHM of the XRD (002) peaks are plotted in Fig. 2(b). The FWHM values decreased from 0.36 to 0.198° as growth temperature increased from 100 to 500°C.

The morphology and the surface roughness determined by AFM measurement are shown in Fig. 6. The roughness seems to increase with a substrate temperature; at the same time, the grain size on the surface also varies. For the film grown at a low temperature (100°C), the grain size is around 90 nm and seems relatively constant. Furthermore, the roughness of this film is about 9 nm. On the contrary, the film grown at a higher temperature (300°C) the grain size of around 115 nm and the roughness of the film slightly decreases to about 8 nm. The sample prepared at up to 500°C

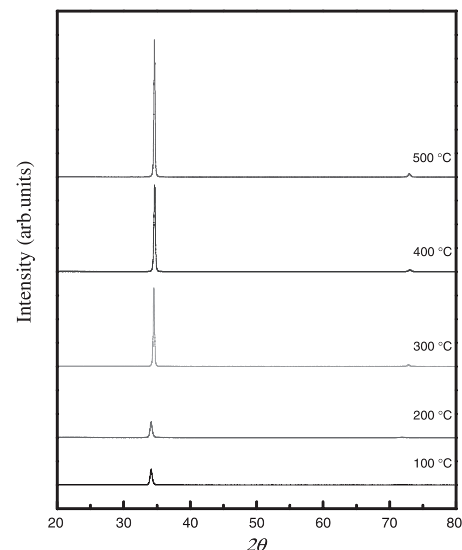

Fig. 5. XRD peaks for different AZO films grown under 5 mTorr of O_2 at various substrate temperatures.

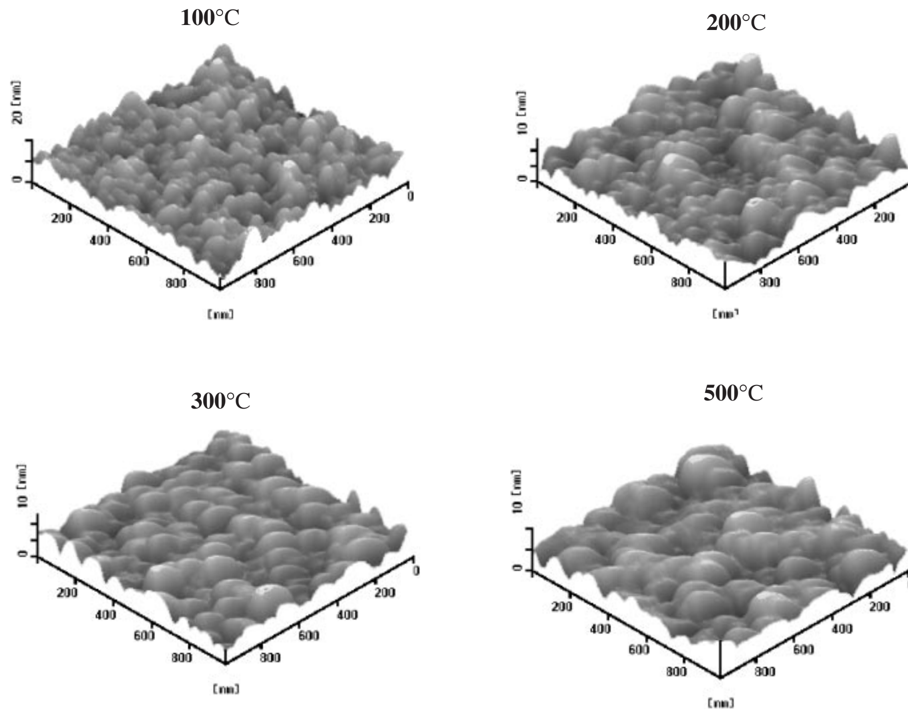

Fig. 6. AFM images of AZO films over $1 \times 1\,\mu m^2$ area grown under 5 mTorr of O_2 at various substrate temperatures.

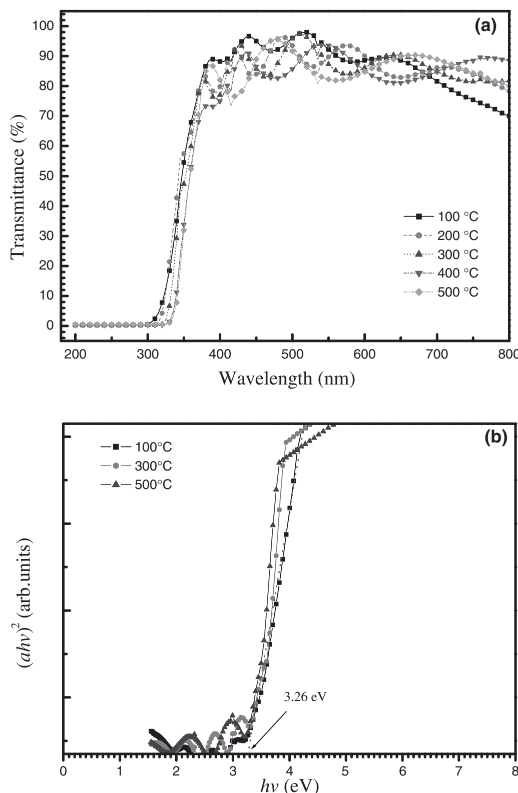

Fig. 7. Optical transmittance (a) for AZO films grown under 5 mTorr of O_2 at various substrate temperatures and Tauc's plot (b).

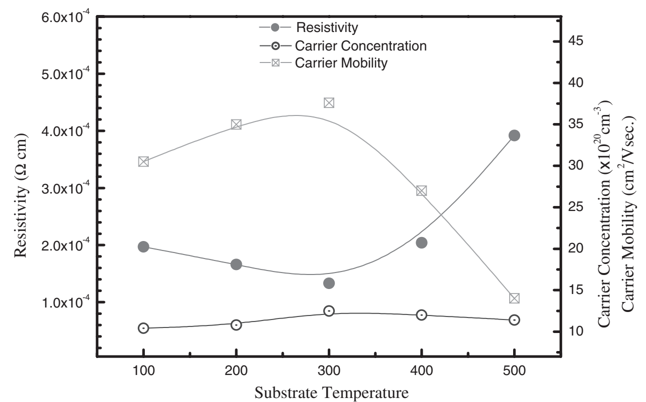

Fig. 8. Figure 4 Variations in resistivity, carrier concentration, and carrier mobility as functions of substrate temperature for AZO films deposited under oxygen pressure of 5 mTorr.

shows a grain size of around 230 nm and a roughness of about 12 nm.

Figure 7 shows the optical transmittance for AZO films grown under 5 mTorr of O_2 at various substrate temperatures. As our goal is to prepare a transparent electrode with a high conductivity for optical applications, a film with a high transmittance in the visible range is very important. The transmittance of AZO films reaches up to 88% in the visible range (400–800 nm), and it decreases slightly from 93 to 88% with an increase in substrate temperature from 100 to 500°C. A conventional ITO electrode has transmittance of about 80%.[20] This indicates that AZO films could transmit more light, and therefore, the AZO film would be a better transparent electrode for display applications. With increasing substrate temperature, the optical band gap is gradually increased from 3.26 to 3.36 eV.

Figure 8 shows the variations in resistivity, carrier concentration and carrier mobility as functions of substrate temperature for the AZO films grown at an oxygen pressure of 5 mTorr. As substrate temperature increases from 100 to 300°C, resistivity decreases from 1.97×10^{-4} to $1.33 \times 10^{-4}\,\Omega\,cm$ and then increases again. The decrease in

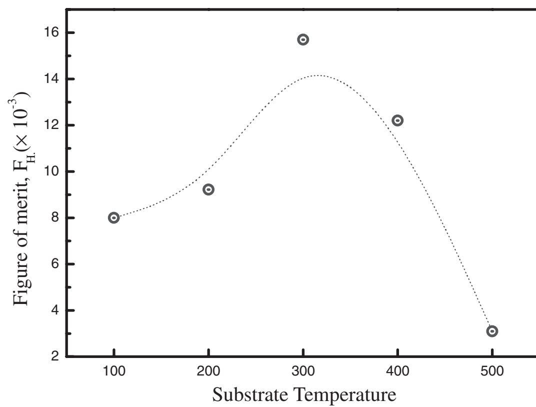

Fig. 9. Variation of figure of merit as a function of substrate temperatures for AZO films deposited under oxygen pressure of 5 mTorr.

resistivity is due to the increase in both carrier concentration and carrier mobility.[21] As substrate temperature increases to 500°C, the corresponding resistivity becomes 3.92×10^{-4} Ω cm. The slight increase in resistivity of the films grown at higher substrate temperatures from 300 to 500°C may be due to contamination of the alkali ions from quartz glass substrates.[22] Carrier concentration in the AZO films was observed to gradually increase as deposition temperature was increased. This increase in carrier concentration may be due to an increase in diffusion of Al atoms from interstitial locations and grain boundaries into the Zn cation sites.[23] Carrier mobility increases from 30.5 $cm^2/(V\,s)$ at to 37.6 $cm^2/(V\,s)$ at substrate temperature of 100 to 300°C, then decreases to 14 $cm^2/(V\,s)$.

In order to investigate the performance of transparent conducting AZO films, the figure of merit (F_H) measured as a function of substrate temperature as shown in Fig. 9. The figure of merit defined by Haacke was considered. F_H is one of the important indices for judging the effectiveness of a process parameter.[24] F_H is defined by

$$F_H\ (\Omega^{-1}) = \frac{T^{10}}{R_s}, \tag{3}$$

where T is the optical transmittance at a specific wavelength ($\lambda = 550$ nm) and R_s is the sheet resistance. It is known that the higher the F_H, the better the quality of the transparent conducting films.[25] Thus, as shown in Fig. 9, the optoelectrical property of AZO films depends on substrate temperature, and the most effective substrate temperature condition at 5 mTorr is 300°C, where F_H is the highest.

4. Conclusions

High-quality transparent conductive AZO thin films were grown using by PLD on quartz glass substrates starting from a ZnO target containing 2 wt% Al_2O_3. The growth was performed in the high oxygen pressure range of 1–100 mTorr and in the substrate temperature range of 100–500°C. We have studied the influence of growth the conditions (oxygen pressure and substrate temperature) on the structural properties that are directly related to the essence of films, such as out-of-plane alignments, in-plane epitaxy, crystal size and grain size. The AZO films formed at a substrate temperature of 300°C showed a low electrical resistivity of 1.33×10^{-4} Ω cm, a carrier concentration of 1.25×10^{21} cm^{-3} and a carrier mobility of 37.6 $cm^2/(V\,s)$ at an oxygen pressure of 5 mTorr. A visible transmittance of above 90% was obtained. The optical band gap of the films increased from 3.26 to 3.36 eV with the increase in substrate temperature from 100 to 500°C. In general, the study indicates that AZO films show comparable electrical and optical properties to those of ITO films and are emerging as a potential good challenger to ITO films.

Acknowledgment

This work is supported in part by a Grant-in-Aid for Scientific Research (2003–V2006, No. 15360171) from the Ministry of Education, Culture, Sports, Science and Technology of Japan.

1) D. G. Thomas: J. Phys. Chem. Solids **15** (1960) 86.
2) M. Joseph, H. Tabata and T. Kawai: Appl. Phys. Lett. **74** (1999) 2534.
3) M. Kon, P. K. Song, Y. Shigesato, P. Frach, S. Ohno and K. Suzuki: Jpn. J. Appl. Phys. **42** (2003) 263.
4) S. Nakamura, M. Senoh, S. Nakahana, N. Iwasa, T. Yamada, T. Matsushita, Y. Sugimoto and H. Kiyoku: Appl. Phys. Lett. **69** (1996) 1477.
5) H. Ohta, K. Kawamura, M. Orita, M. Hirano, N. Sarukura and H. Hosono: Appl. Phys. Lett. **77** (2000) 475.
6) P. F. Carcia, R. S. McLean, M. H. Reilly and G. Nunes: Appl. Phys. Lett. **82** (2003) 1117.
7) G. J. Exarhos and S. K. Sharma: Thin Solid Films **270** (1995) 27.
8) K. Tominaga, M. Kataoka, H. Manabe, T. Ueda and I. Mory: Thin Solid Films **290–291** (1996) 84.
9) K. Matsubara, P. Fons, K. Iwata, A. Yamada, K. Sakurai, H. Tampo and S. Niki: Thin Solid Films **431–432** (2003) 369.
10) H. Kim, C. M. Gilmore, J. S. Horwitz, A. Pique, H. Murata, G. P. Kushto, R. Schlaf, Z. H. Kafafi and D. B. Chrisey: Appl. Phys. Lett. **76** (2000) 259.
11) J. S. Selvan, M. Fujimura and T. Suhara: Jpn. J. Appl. Phys. **43** (2004) 5313.
12) S. Suzuki, T. Miyata, M. Ishii and T. Minami: Thin Solid Film **434** (2003) 14.
13) Y. Natsume and H. Sakata: Mater. Chem. Phys. **78** (2002) 170.
14) T. Ohshima, T. Ikegami, K. Ebihara, J. Asmussen and R. K. Thareja: Thin Soild Films **435** (2003) 49.
15) D. B. Chrisey and G. K. Hubler: *Pulsed Laser Deposition of Thin Films* (Wiley, New York, 1994) p. 327.
16) T. Ohshima, R. K. Thareja, T. Ikegami, K. Ebihara and J. Narayan: Sci. Technol. Adv. Mater. **2** (2001) 517.
17) S. Choopum, R. D. Vispute, W. Zoch, A. Balsamo, R. P. Sharma, T. Venkatesan, A. Iliadis and D. C. Lock: Appl. Phys. Lett. **75** (1999) 3947.
18) J. Ma, F. Jin, D.-H. Zhang, H.-L. Ma and S.-Y. Li: Thin Solid Films **357** (1999) 98.
19) T. Makino, K. Tamura, C. H. Chia, Y. Segawa, M. Kawasaki, A. Ohtomo and H. Koinuma: Phys. Rev. B **65** (2002) 121201(R).
20) S. Seki, M. Ogawa and Y. Sawada: Jpn. J. Appl. Phys. **40** (2001) L1244.
21) A. Suzuki, T. Matsushita, N. Wada, Y. Sakamoto and M. Okuda: Jpn. J. Appl. Phys. **35** (1996) L56.
22) J. C. Manifacier: Thin Solid Films **90** (1982) 297.
23) H. Kim, C. M. Gilmore, A. Pique, J. S. Horwitz, H. Mattoussi, H. Murata, Z. H. Kafai and D. B. Chrisey: J. Appl. Phys. **86** (1999) 6451.
24) G. Haacke: J. Appl. Phys. **47** (1976) 4086.
25) S. Ray, R. Banerjee, N. Basu, A. Batabyal and A. Barua: J. Appl. Phys. **54** (1983) 3497.